

On Model Selection Consistency of Lasso for High-Dimensional Ising Models on Tree-like Graphs

Xiangming Meng^{*1}, Tomoyuki Obuchi² and Yoshiyuki Kabashima¹

¹Institute for Physics of Intelligence and Department of Physics, Graduate School of Science, The University of Tokyo, Tokyo, Japan

²Department of Systems Science, Graduate School of Informatics, Kyoto University, Kyoto, Japan

October 19, 2021

Abstract

We consider the problem of high-dimensional Ising model selection using neighborhood based least absolute shrinkage and selection operator (Lasso). It is rigorously proved that under some mild coherence conditions on the population covariance matrix of the Ising model, consistent model selection can be achieved with sample sizes $n = \Omega(d^3 \log p)$ for any tree-like graph in the paramagnetic phase, where p is the number of variables and d is the maximum node degree. When the same conditions are imposed directly on the sample covariance matrices, it is shown that a reduced sample size $n = \Omega(d^2 \log p)$ suffices. The obtained sufficient conditions for consistent model selection with Lasso are the same in the scaling of the sample complexity as that of ℓ_1 -regularized logistic regression. Given the popularity and efficiency of Lasso, our rigorous analysis provides a theoretical backing for its practical use in Ising model selection.

1 Introduction

Undirected graphical models, also widely known as Markov random fields (MRFs), are a powerful tool for modeling high dimensional probability distributions. The conditional independence relationships between random variables can be well captured by the associated graphs [Koller and Friedman, 2009, Wainwright and Jordan, 2008]. It is thus of significant importance to reconstruct the underlying graph structure of the MRFs from independent, identically distributed (i.i.d.) random samples. With the recent advent of massive data,

^{*}E-mail: meng@g.ecc.u-tokyo.ac.jp

the problem of learning graph structure of MRFs, also termed as graphical model selection, has attracted a surge of interests in various scientific disciplines such as image analysis [Roth and Black, 2005], social networking [McAuley and Leskovec, 2012, Perc et al., 2017], gene network analysis [Krishnan et al., 2020, Marbach et al., 2012], and protein interactions [Liebl and Zacharias, 2021, Morcos et al., 2011], just to name a few.

Among various kinds of MRFs, the Ising model [Ising, 1925] is the most renowned binary graphical model with pairwise interaction potentials [Mezard and Montanari, 2009, Wainwright and Jordan, 2008]. The problem of Ising model selection, i.e., reconstructing the graph structure of an Ising model from i.i.d. samples, has been studied extensively and various methods have been proposed. As the Ising model is originally proposed in statistical physics [Ising, 1925], some early attempts for Ising model selection are heuristic mean-field methods from the physics community [Kappen and Rodríguez, 1998, Ricci-Tersenghi, 2012, Tanaka, 1998]. However, methods utilizing mean-field approximations perform poorly for Ising models with long-range correlations. To address this problem and further improve the performance, a variety of methods have been proposed in the past years [Decelle and Ricci-Tersenghi, 2014, Höfling and Tibshirani, 2009, Lokhov et al., 2018, Ravikumar et al., 2010, Vuffray et al., 2016, Wainwright et al., 2007]. Notably, under the framework of the pseudo-likelihood (PL) method [Besag, 1975], the statistical community has provided a strong theoretical backing for ℓ_1 -regularized logistic regression (ℓ_1 -LogR) [Ravikumar et al., 2010]. In addition, the regularized interaction screening estimator (RISE) is proposed in Vuffray et al. [2016] using a local cost function called interaction screening objective (ISO) (a logarithmic version is proposed in Lokhov et al. [2018]). It has been theoretically demonstrated that the RISE requires a number of samples that is near-optimal with respect to (w.r.t.) previously established information-theoretic lower-bound [Santhanam and Wainwright, 2012]. Interestingly, both the ℓ_1 -LogR and RISE estimators belong to the common framework of ℓ_1 -regularized M-estimators [Negahban et al., 2012] but only with different loss functions. The use of logistic loss in ℓ_1 -LogR [Ravikumar et al., 2010] stems from its consistency with the underlying conditional likelihood of the Ising model while the ISO loss in RISE is specially designed according to the physical “interaction screening” property [Lokhov et al., 2018, Vuffray et al., 2016].

In practice, however, the underlying model generating the observed samples is usually unknown *a priori*, i.e., model mismatch or misspecification is inevitable and thus in general it is difficult to obtain a loss function consistent with the true conditional likelihood as ℓ_1 -LogR [Ravikumar et al., 2010], nor is it easy to design a specific ISO satisfying the “interaction screening” property as RISE [Lokhov et al., 2018, Vuffray et al., 2016]. Consequently, one natural question is that, is it still possible to recover the structure of the Ising model using a misspecified loss function such as the quadratic loss? To the best of our knowledge, this problem has not been rigorously studied, though there are several recent non-rigorous works in the statistical physics literature [Abbara et al., 2020, Meng et al., 2020, 2021]. In particular, it is shown in Meng et al. [2021] that even in the case with a misspecified quadratic loss, the neighborhood-based least absolute shrinkage and selection

operator (Lasso) [Tibshirani, 1996] (termed as ℓ_1 -regularized linear regression (ℓ_1 -LinR) in Meng et al. [2021]) has the same order of sample complexity as ℓ_1 -LogR for random regular (RR) graphs in the whole paramagnetic phase [Mezard and Montanari, 2009]. Furthermore, Meng et al. [2021] provides an accurate estimate of the typical sample complexity as well as a precise prediction of the non-asymptotic learning performance. However, there are several limitations in Meng et al. [2021]. First, since the replica method [Mezard and Montanari, 2009, Mézard et al., 1987, Nishimori, 2001, Opper and Saad, 2001] they use is a non-rigorous method from statistical mechanics, a rigorous mathematical proof is lacking. Second, the results in Meng et al. [2021] are restricted to the ensemble of RR graphs since the obtained equations of state (EOS) explicitly depend on the eigenvalue distribution (EVD) of the covariance matrix, which is intractable for general graphs. In addition, since their analysis relies on the *self averaging property* [Mezard and Montanari, 2009, Nishimori, 2001], the results in Meng et al. [2021] are meaningful in terms of the “*typical case*” rather than the worst case. Another closely related work is Lokhov et al. [2018], which states that at high temperatures when the magnitudes of the couplings are approaching zero, both logistic and IOS losses can be approximated by a quadratic loss using the second-order Taylor expansion, so that both the ℓ_1 -LogR and RISE estimators behave similarly as the Lasso estimator at high temperatures. However, a rigorous analysis of the Lasso estimator itself is still lacking. Moreover, although the Taylor expansion is used in Lokhov et al. [2018] to illustrate the similarity between Lasso and ℓ_1 -LogR/RISE, there is no quantitative analysis of the exact valid regime for the success of Lasso, especially when no post-thresholding is performed.

In this paper, we provide a rigorous proof of the model selection consistency of Lasso for high-dimensional Ising models on any tree-like graphs in the whole paramagnetic phase [Mezard and Montanari, 2009]. Our proof builds on the framework of the primal-dual witness method in Ravikumar et al. [2010] for ℓ_1 -LogR but with several key modifications specially tailored to the Lasso estimator. Specifically, there are two crucial differences between the quadratic loss of Lasso and logistic/ISO losses of ℓ_1 -LogR/RISE [Ravikumar et al., 2010, Vuffray et al., 2016]. First, the solution to the zero-gradient condition of the expected quadratic loss is no longer the true parameter vector but a rescaled one. Second, the Hessian matrix of the expected quadratic loss reduces to the covariance matrix. Interestingly, such differences on the one hand simplify the analysis somewhere while on the other hand complicate the analysis elsewhere but overall, remarkably, it leads to the same scaling of the sample complexity as the ℓ_1 -LogR estimator [Ravikumar et al., 2010] for consistent Ising model selection. Specifically, our main results show that under mild assumptions on the population covariance matrix, consistent Ising model selection can be achieved using $\Omega(d^3 \log p)$ samples with Lasso for any paramagnetic tree-like graphs, where p is the number of variables of the Ising model and d is the maximum node degree. When the same assumptions are directly imposed on the sample covariance matrices, only $\Omega(d^2 \log p)$ samples suffice. Compared to previous works [Lokhov et al., 2018, Meng et al., 2021], we provide a rigorous analysis of Lasso for Ising model selection and explicitly prove its

consistency in the whole paramagnetic phase. Given the wide popularity and efficiency of Lasso, such rigorous analysis provides a theoretical backing for its practical use in Ising model selection, which can be viewed as a complement to that for Gaussian graphical models [Meinshausen et al., 2006, Zhao and Yu, 2006].

The remainder of this paper is organized as follows. In section 2, we first provide a background of the Ising model and the problem setup. Section 3 states the main results. Section 4 gives the proof of the main results. In Section 5, numerical simulations are conducted to verify the theoretical analysis. Finally, Section 6 concludes the paper with some discussions.

2 Background and Problem Setup

We begin with some background on the Ising model, the definition of the Ising model selection, and an introduction to the neighborhood-based Lasso estimator. We follow the notations of Ravikumar et al. [2010] very closely for ease of comparison.

2.1 Ising Model

The Ising model is one classical graphical model originated from statistical physics [Ising, 1925], which is one special class of MRFs with pairwise potentials and each variable takes binary values $\{-1, +1\}$ [Mezard and Montanari, 2009, Opper and Saad, 2001]. The joint probability distribution of an Ising model with p variables (spins) $X = (X_i)_{i=1}^p$ has the following form

$$\mathbb{P}_{\theta^*}(x) = \frac{1}{Z(\theta^*)} \exp \left\{ \sum_{r \neq t} \theta_{rt}^* x_r x_t \right\}, \quad (1)$$

where $Z(\theta^*) = \sum_x \exp \left\{ \sum_{r \neq t} \theta_{rt}^* x_r x_t \right\}$ is the partition function and $\theta^* = (\theta_{rt}^*)_{r \neq t}$ is the coupling vector, respectively. In general, there are also external fields but here they are assumed to be zero for simplicity. The structure of an Ising model can be described by an undirected graph $G = (V, E)$, where $V = \{1, \dots, p\}$ is a collection of the indices of the vertices X of the graph, and $E = \{(r, t) | \theta_{rt}^* \neq 0\}$ is a collection of undirected edges. For each vertex $r \in V$, its neighborhood set is defined as the subset $\mathcal{N}(r) := \{t \in V | (r, t) \in E\}$ and the corresponding node degree is given by $d_r := |\mathcal{N}(r)|$. The maximum node degree of the graph G is denoted as $d := \max_{r \in V} d_r$. We use $\mathcal{G}_{p,d}$ to denote the ensemble of graphs G with p vertices and maximum (not necessarily bounded) node degree $d \geq 3$. The minimum and maximum magnitudes of the couplings θ_{rt}^* for $(r, t) \in E$ are respectively defined as

$$\theta_{\min}^* := \min_{(r,t) \in E} |\theta_{rt}^*|, \quad \theta_{\max}^* := \max_{(r,t) \in E} |\theta_{rt}^*|. \quad (2)$$

Regarding the specific structure of the graph $G \in \mathcal{G}_{p,d}$, various types exist and in this paper we specially focus on the ensemble of tree-like graphs, which serves as one assumption for proving the consistency of Lasso as illustrated in assumption (A3) in Sec. 3.1.

2.2 Ising Model Selection

The problem of Ising model selection refers to recovering the underlying graph structure (edge set E) of graph G from a collection of n i.i.d. samples $\mathfrak{X}_1^n := \{x^{(1)}, \dots, x^{(n)}\}$ of the Ising model, where $x^{(i)} \in \{-1, +1\}^p$ represents the i -th sample. As in Ravikumar et al. [2010], we consider the slightly stronger criterion of *signed* edge recovery. Specifically, given one Ising model with couplings θ^* and edge set E , the edge sign vector E^* is defined as follows [Ravikumar et al., 2010]

$$E^* = \begin{cases} \text{sign}(\theta_{rt}^*), & \text{if } (r, t) \in E; \\ 0, & \text{otherwise,} \end{cases} \quad (3)$$

where $\text{sign}(\cdot)$ is an element-wise operation that maps every positive entry to 1, negative entry to -1, and zero entry to zero. Suppose that \hat{E}_n is an estimator of the edge sign vector E^* given \mathfrak{X}_1^n , then correct signed edge recovery is achieved if and only if $\hat{E}_n = E^*$.

In this paper, we are interested in Ising model selection in the high dimensional ($n \ll p$) regime, where both the number of vertices $p = p(n)$ and the maximum node degree $d = d(n)$ may also scale as a function of the sample size n . Our goal is to investigate the sufficient conditions on the scaling of (n, p, d) so that the considered neighborhood-based Lasso estimator (as described in Sec. 2.3) is *model selection consistent* in the sense that

$$\mathbb{P}(\hat{E}_n = E^*) \rightarrow 1 \text{ as } n \rightarrow +\infty, \quad (4)$$

which is also known as the *sparsistency* property [Ravikumar et al., 2010].

2.3 Neighborhood-based Lasso

The problem of graph structure recovery can be divided into a parallel of sub-problems for each vertex $r \in V$. This is justified by the fact that for any graph $G = (V, E)$, recovering the edge sign vector E^* (3) is equivalent to recovering the associated neighborhood set $\mathcal{N}(r)$ for each vertex $r \in V$ along with its correct signs $\text{sign}(\theta_{rt}^*)$ for every $t \in \mathcal{N}(r)$ [Ravikumar et al., 2010]. For each vertex $r \in V$, the signed neighborhood set is defined as

$$\mathcal{N}_{\pm}(r) := \{\text{sign}(\theta_{rt}^*) t \mid t \in \mathcal{N}(r)\}. \quad (5)$$

Denote $\theta_{\setminus r}^* := \{\theta_{rt}^* \mid t \in V \setminus r\} \in \mathbb{R}^{p-1}$ as the sub-vector associated with the vertex $r \in V$. Suppose that $\hat{\theta}_{\setminus r}$ is an estimator of $\theta_{\setminus r}^*$, then one can estimate the signed neighbor-

hood $\hat{\mathcal{N}}_{\pm}(r)$ from $\hat{\theta}_{\setminus r}$. Consequently, the event $\{\hat{E}_n = E^*\}$ is equivalent to the event $\{\hat{\mathcal{N}}_{\pm}(r) = \mathcal{N}_{\pm}(r), \forall r \in V\}$, i.e., every signed neighborhood set is recovered correctly. Note that, given the estimator $\hat{\theta}_{\setminus r}$, there are various methods to estimate the signed neighborhood $\hat{\mathcal{N}}_{\pm}(r)$. In this paper, similar to Ravikumar et al. [2010], we consider estimating $\hat{\mathcal{N}}_{\pm}(r)$ as follows

$$\hat{\mathcal{N}}_{\pm}(r) := \left\{ \text{sign} \left(\hat{\theta}_{rt} \right) t \mid t \in V \setminus r, \hat{\theta}_{rt} \neq 0 \right\}. \quad (6)$$

Alternatively, one can also introduce a threshold and then perform post-thresholding as Lokhov et al. [2018], Vuffray et al. [2016]. Here, we only focus on the case without post-thresholding.

Then, the main goal is to obtain the estimator $\hat{\theta}_{\setminus r}$. There are several popular nonlinear estimators such as ℓ_1 -LogR [Ravikumar et al., 2010] and RISE [Vuffray et al., 2016]. In this paper we consider one simple linear estimator, i.e., the neighborhood-based Lasso estimator. Specifically, for each vertex $r \in V$, the estimator $\hat{\theta}_{\setminus r}$ is obtained as follows

$$\hat{\theta}_{\setminus r} = \arg \min_{\theta_{\setminus r}} \left\{ \ell(\theta_{\setminus r}; \mathfrak{X}_1^n) + \lambda_{(n,p,d)} \|\theta_{\setminus r}\|_1 \right\}, \quad (7)$$

where $\ell(\theta_{\setminus r}; \mathfrak{X}_1^n)$ denotes the quadratic loss function

$$\ell(\theta_{\setminus r}; \mathfrak{X}_1^n) := \frac{1}{2n} \sum_{i=1}^n \left(x_r^{(i)} - \sum_{u \in V \setminus r} \theta_{ru} x_u^{(i)} \right)^2, \quad (8)$$

and $\lambda_{(n,p,d)} > 0$ is the regularization parameter, which might depend on the value of (n, p, d) . For notational simplicity, instead of $\lambda_{(n,p,d)}$, λ_n will be used hereafter. Our main concern is the scaling condition on (n, p, d) which ensures that the estimated signed neighborhood $\hat{\mathcal{N}}_{\pm}(r)$ in (6) agrees with the true neighborhood, i.e., $\{\hat{\mathcal{N}}_{\pm}(r) = \mathcal{N}_{\pm}(r), \forall r \in V\}$, with high probability.

3 Main results

3.1 Assumptions

Similar to Ravikumar et al. [2010], the success of the neighborhood-based Lasso estimator (7) relies on several assumptions. First, as Ravikumar et al. [2010], we introduce the *dependency condition* and *incoherence condition* for the Hessian of the expected square loss $\mathbb{E}_{\theta^*} \{\ell(\theta; \mathfrak{X}_1^n)\}$, where $\mathbb{E}_{\theta^*} \{\cdot\}$ denotes expectation w.r.t. the joint distribution $\mathbb{P}_{\theta^*}(x)$ in (1). However, different from the case of logistic loss in Ravikumar et al. [2010], the Hessian of $\mathbb{E}_{\theta^*} \{\ell(\theta; \mathfrak{X}_1^n)\}$ with quadratic loss (8) corresponds to the covariance matrix of

$X_{\setminus r}$, which is independent of the value of θ and hence the additional variance function term in Ravikumar et al. [2010] does not exist. Specifically, for each fixed vertex $r \in V$, the Hessian of $\mathbb{E}_{\theta^*} \{\ell(\theta; \mathfrak{X}_1^n)\}$ is a $(p-1) \times (p-1)$ matrix of the form

$$Q_r^* := \mathbb{E}_{\theta^*} \{\nabla^2 \ell(\theta; \mathfrak{X}_1^n)\} = \mathbb{E}_{\theta^*} \{X_{\setminus r} X_{\setminus r}^T\}. \quad (9)$$

For notational simplicity, Q_r^* will be written as Q^* hereafter. Denote $S := \{(r, t) \mid t \in \mathcal{N}(r)\}$ as the subset of indices associated with edges of r and S^c as its complement. The $d_r \times d_r$ sub-matrix of Q^* indexed by S is denoted as Q_{SS}^* , where d_r is the node degree of node r . The *dependency condition* and *incoherence condition* are described as follows.

Assumption 1 (A1): *dependency condition*. The sub-matrix Q_{SS}^* has bounded eigenvalue, i.e., there exists a finite constant $C_{\min} > 0$ such that

$$\Lambda_{\min}(Q_{SS}^*) \geq C_{\min}. \quad (10)$$

Assumption 2 (A2): *incoherence condition*. There exists an $\alpha \in (0, 1]$ such that

$$\| \| Q_{S^c S}^* (Q_{SS}^*)^{-1} \| \|_{\infty} \leq 1 - \alpha, \quad (11)$$

where $\| \| A \| \|_{\infty} = \max_j \sum_k |A_{jk}|$ is the ℓ_{∞} matrix norm of a matrix A .

Compared to the ℓ_1 -LogR estimator [Ravikumar et al., 2010], the assumptions (A1) and (A2) for the neighborhood-based Lasso (7) are easier to check since they are only imposed on the covariance matrix. Besides, it is assumed that the graph is tree-like and in the paramagnetic phase.

Assumption 3 (A3): *Paramagnetic tree-like graph condition*. The underlying graph $G \in \mathcal{G}_{p,d}$ of the Ising model is assumed to be a sparse tree-like graph in the paramagnetic phase [Mezard and Montanari, 2009].

This sparse tree-like assumption implies that the loops in the graph can be neglected and the corresponding free energy can be described by the so-called Bethe free energy [Mezard and Montanari, 2009]. The paramagnetic phase assumption indicates that the Ising model is above the critical temperature so that the spontaneous magnetization is zero [Mezard and Montanari, 2009, Nishimori, 2001]. Note that for RR graphs, under the assumption (A3), assumptions (A1) and (A2) naturally hold, as shown in Proposition 1.

Proposition 1 *For a RR graph with uniform coupling strength θ_0 and constant node degree d , the dependency condition in (A1) and incoherence condition in (A2) naturally hold under the assumption (A3).*

Proof See Appendix B. ■

It is conjectured that the assumption (A3) is not essential for consistent model selection, though it is necessary for the proof below. In fact, as can be seen from the numerical

experiments in Section 5 that, even for graphs with many loops such as the square lattice, the reconstruction probability of the Lasso estimator behaves essentially similarly to tree-like graphs. We here leave relaxing the assumption (A3) as future work.

3.2 Statement of main results

First consider the case of “fixed design” of the sample covariance matrices

$$Q^n := \frac{1}{n} \sum_{i=1}^n X_{\setminus r}^{(i)} \left(X_{\setminus r}^{(i)} \right)^T, \quad (12)$$

which satisfy the assumptions (A1) and (A2). Similar to Ravikumar et al. [2010], we define the “good event” as follows

$$\mathcal{M} := \{ \mathfrak{X}_1^n \in \{-1, +1\}^{n \times p} \mid Q^n \text{ satisfies (A1) and (A2)} \}. \quad (13)$$

Then, when the original Ising model satisfies (A3), we have Theorem 1.

Theorem 1 (*fixed design*) *Consider an Ising model defined on a graph $G = (V, E) \in \mathcal{G}_{p,d}$ with parameter vector θ^* and associated sign edge set E^* such that the assumption (A3) is satisfied. Suppose that the event \mathcal{M} holds and the regularization parameter λ_n is selected to satisfy $\lambda_n \geq \frac{4\sqrt{c+1}(2-\alpha)}{\alpha} \sqrt{\frac{\log p}{n}}$ for some constant $c > 0$. Under these conditions, if*

$$n \geq (c+1)d^2 \log p, \quad (14)$$

then with probability at least $1 - 2 \exp(-c \log p) \rightarrow 1$ as $p \rightarrow \infty$, the following properties hold:

(a) *For each node $r \in V$, the Lasso estimator (7) has a unique solution, and thus uniquely specifies a signed neighborhood $\hat{\mathcal{N}}_{\pm}(r)$.*

(b) *For each node $r \in V$, the estimated signed neighborhood vector $\hat{\mathcal{N}}_{\pm}(r)$ correctly excludes all edges not in the true neighborhood. Moreover, it correctly includes all edges if $\tilde{\theta}_{\min}^* \geq \frac{6\lambda_n \sqrt{d}}{C_{\min}}$, where $\tilde{\theta}_{\min}^*$ is the minimum magnitude of the rescaled parameter $\tilde{\theta}^*$ and is defined later in (34).*

Theorem 1 indicates that, remarkably, under some mild assumptions (A1) and (A2) on sample covariance matrices, in the high-dimensional setting (for $p \rightarrow \infty$), the Lasso estimator is model selection consistent with $n = \Omega(d^2 \log p)$ samples for tree-like Ising models in the paramagnetic phase. Note that minimum magnitude of the rescaled parameter $\tilde{\theta}^*$ might be difficult to evaluate for general graphs. Instead, a relaxed condition can be obtained by using a lower bound of $\tilde{\theta}_{\min}^*$ (see Appendix A). In the case of RR graphs with coupling strength θ_0 and node degree d , it can be easily obtained as $\tilde{\theta}_{\min}^* = \frac{\tanh(\theta_0)}{1+(d-1)\tanh^2(\theta_0)}$.

In Theorem 1, the assumptions (A1) and (A2) are directly imposed on the sample covariance matrices Q^n . When (A1) and (A2) are imposed on the population covariance matrix Q^* , we obtain the following Theorem 2.

Theorem 2 *Consider an Ising model defined on a graph $G = (V, E) \in \mathcal{G}_{p,d}$ with parameter vector θ^* and associated sign edge set E^* such that assumption (A3) is satisfied. Moreover, assumptions (A1) and (A2) are satisfied by the population covariance matrix Q^* . Suppose that the regularization parameter λ_n is selected to satisfy $\lambda_n \geq \frac{4\sqrt{c+1}(2-\alpha)}{\alpha} \sqrt{\frac{\log p}{n}}$ for some constant $c > 0$. Then there exists a constant L independent of (n, p, d) such that if*

$$n \geq Ld^3 \log p, \tag{15}$$

then with probability at least $1 - 2 \exp(-c \log p) \rightarrow 1$ as $p \rightarrow \infty$, the following properties hold:

(a) For each node $r \in V$, the Lasso estimator (7) has a unique solution, and thus uniquely specifies a signed neighborhood $\hat{N}_\pm(r)$.

(b) For each node $r \in V$, the estimated signed neighborhood vector $\hat{N}_\pm(r)$ correctly excludes all edges not in the true neighborhood. Moreover, it correctly includes all edges if the minimum magnitude of the rescaled parameter satisfies $\tilde{\theta}_{\min}^* \geq \frac{6\lambda_n \sqrt{d}}{C_{\min}}$.

Theorem 2 indicates that, if the same assumptions (A1) and (A2) are imposed on the population covariance matrix Q^* , then in the high-dimensional setting (for $p \rightarrow \infty$), the Lasso estimator is model selection consistent with $n = \Omega(d^3 \log p)$ samples for any tree-like Ising models in the paramagnetic phase.

4 Proof of the Main Results

In this section, we present the detailed proofs of Theorem 1 and Theorem 2, respectively.

4.1 Sketch of the proof

Our proofs of Theorem 1 and Theorem 2 follow closely the one in Ravikumar et al. [2010]. First, we prove Theorem 1 for fixed-design of the sample covariance matrices $Q^n := \frac{1}{n} \sum_i X_{\setminus r}^{(i)} \left(X_{\setminus r}^{(i)} \right)^T$. Then, it is demonstrated that imposing the dependence condition (A1) and incoherence condition (A2) on the population covariance matrices $Q_r^* := \mathbb{E}_{\theta^*} \left\{ X_{\setminus r} X_{\setminus r}^T \right\}$ guarantees that the associated conditions hold for the sample covariance matrices with high probability. Given Theorem 1, the proof of Theorem 2 is the same as that of Ravikumar et al. [2010] using some large-deviation analysis. Thus our main focus is the proof of Theorem 1 which, due to the misspecified quadratic loss, requires several key modifications of the result in Ravikumar et al. [2010].

As in Ravikumar et al. [2010], we use the primal-dual witness proof framework. The main idea of the primal-dual witness method is to explicitly construct an optimal primal-dual pair which satisfies the sub-gradient optimality conditions associated with the ℓ_1 -regularized estimator (in our case it is the Lasso estimator (7)). Subsequently, we prove that under the stated assumptions on (n, p, d) , the optimal primal-dual pair can be constructed such that they act as a witness, i.e., a certificate that guarantees that the neighborhood-based Lasso estimator correctly recovers the sign edge set of the graph $G \in \mathcal{G}_{p,d}$.

Specifically, for each vertex $r \in V$, an optimal primal-dual pair $(\hat{\theta}_{\setminus r}, \hat{z}_r)$ is constructed, where $\hat{\theta}_{\setminus r} \in \mathbb{R}^{p-1}$ is a primal solution and $\hat{z}_r \in \mathbb{R}^{p-1}$ is the associated sub-gradient vector. They satisfy the zero sub-gradient optimality condition [Rockafellar, 1970] associated with the Lasso estimator (7):

$$\nabla \ell(\hat{\theta}_{\setminus r}; \mathfrak{X}_1^n) + \lambda_n \hat{z}_r = 0, \quad (16)$$

where the sub-gradient vector \hat{z}_r satisfies

$$\begin{cases} \hat{z}_{rt} = \text{sign}(\hat{\theta}_{rt}), \text{ if } \hat{\theta}_{rt} \neq 0; & (a) \\ |\hat{z}_{rt}| \leq 1, \text{ otherwise.} & (b) \end{cases} \quad (17)$$

Then, the pair is a primal-dual optimal solution to (7) and its dual. Further, to ensure that such an optimal primal-dual pair correctly specifies the signed neighborhood of node r , the sufficient and necessary conditions are as follows

$$\begin{cases} \text{sign}(\hat{z}_{rt}) = \text{sign}(\theta_{rt}^*), \forall (r, t) \in S := \{(r, t) \mid (r, t) \in E\}, & (a) \\ \hat{\theta}_{ru} = 0, \forall (r, u) \in S^c := E \setminus S. & (b) \end{cases} \quad (18)$$

Note that while the regression in (7) corresponds to a convex problem, for $p \gg n$ in the high-dimensional regime, it is not necessarily strictly convex so that there might be multiple optimal solutions. Fortunately, the following lemma in Ravikumar et al. [2010] provides sufficient conditions for shared sparsity among optimal solutions as well as uniqueness of the optimal solution.

Lemma 1 (Lemma 1 in Ravikumar et al. [2010]). *Suppose that there exists an optimal primal solution $\hat{\theta}_{\setminus r}$ with associated optimal dual vector \hat{z}_r such that $\|\hat{z}_{S^c}\|_\infty < 1$. Then any optimal primal solution $\tilde{\theta}$ must have $\tilde{\theta}_{S^c} = 0$. Moreover, if the Hessian sub-matrix $[\nabla^2 \ell(\hat{\theta}_{\setminus r}; \mathfrak{X}_1^n)]_{SS}$ is strictly positive definite, then $\hat{\theta}_{\setminus r}$ is the unique optimal solution.*

According to Lemma 1, following Ravikumar et al. [2010], we can construct a primal-dual witness $(\hat{\theta}_{\setminus r}, \hat{z})$ for the Lasso estimator (7) as follows:

(a) First, set $\hat{\theta}_S$ as the minimizer of the partial penalized likelihood

$$\hat{\theta}_S = \arg \min_{\theta_{\setminus r} = (\theta_S, 0) \in \mathbb{R}^{p-1}} \{ \ell(\theta_{\setminus r}; \mathfrak{X}_1^n) + \lambda_n \|\theta_S\|_1 \}, \quad (19)$$

and then set $\hat{z}_S = \text{sign}(\hat{\theta}_S)$.

(b) Second, set $\hat{\theta}_{S^c} = 0$ so that condition (18) (b) holds.

(c) Third, obtain \hat{z}_{S^c} from (16) by substituting the values of $\hat{\theta}_{\setminus r}$ and \hat{z}_S .

(d) Finally, we need to show that the stated scalings of (n, p, d) imply that, with high probability, the remaining conditions (18) (a) and (17) are satisfied.

Similar to Ravikumar et al. [2010], our analysis in step (d) demonstrates that $\|\hat{z}_{S^c}\|_\infty < 1$ with high probability. Furthermore, under the conditions of Theorem 1, the sub-matrix of the sample covariance matrices are strictly positive definite with high probability so that, by Lemma 1, it is guaranteed that the primal solution $\hat{\theta}_{\setminus r}$ is unique.

4.2 Some key results

Some key technical results central to the proof are presented in this subsection. First, we obtain the zero-gradient solution to $\mathbb{E}_{\theta^*}(\nabla \ell(\theta_{\setminus r}; \mathfrak{X}_1^n)) = 0$ for the quadratic loss (8).

Lemma 2 *For a tree-like graph in the paramagnetic phase (assumption (A3)), the solution to $\mathbb{E}_{\theta^*}(\nabla \ell(\theta_{\setminus r}; \mathfrak{X}_1^n)) = 0$, denoted as $\tilde{\theta}_{\setminus r}^* = \left\{ \tilde{\theta}_{rt}^* \right\}_{t \in V \setminus r} \in \mathbb{R}^{p-1}$, can be obtained as*

$$\tilde{\theta}_{rt}^* = \begin{cases} \frac{1}{1-d_r + \sum_{u \in \mathcal{N}(r)} \frac{1}{1-\tanh^2(\theta_{ru}^*)}} \frac{\tanh(\theta_{rt}^*)}{1-\tanh^2(\theta_{rt}^*)} & \text{if } (r, t) \in E; \\ 0 & \text{otherwise.} \end{cases} \quad (20)$$

In particular, for RR graphs with constant coupling strength $|\theta_{rt}^| = \theta_0 > 0, \forall (r, t) \in E$ and degree node $d_r = d$, there is*

$$\tilde{\theta}_{rt}^* = \begin{cases} \frac{\tanh(\theta_0) \text{sign}(\theta_{rt}^*)}{1+(d-1)\tanh^2(\theta_0)} & \text{if } (r, t) \in E; \\ 0 & \text{otherwise.} \end{cases} \quad (21)$$

Proof The gradient of the quadratic loss $\ell(\theta_{\setminus r}; \mathfrak{X}_1^n)$ in (8) w.r.t. $\theta_{\setminus r}$ reads

$$\nabla \ell(\theta_{\setminus r}; \mathfrak{X}_1^n) = \frac{1}{n} \sum_{i=1}^n x_{\setminus r}^{(i)} \left(x_r^{(i)} - \sum_{t \in V \setminus r} \theta_{rt} x_t^{(i)} \right). \quad (22)$$

After taking expectation of gradient $\nabla \ell(\theta_{\setminus r}; \mathfrak{X}_1^n)$ over the distribution $\mathbb{P}_{\theta^*}(x)$ and setting

it to be zero, we obtain $\mathbb{E}_{\theta^*} (\nabla \ell (\theta_{\setminus r}; \mathfrak{X}_1^n)) = 0$ in matrix form:

$$Q_r^* \theta_{\setminus r} = b, \quad (23)$$

where $Q_r^* = \mathbb{E}_{\theta^*} (X_{\setminus r} X_r^T)$ is the covariance matrix of $X_{\setminus r}$ and $b = \mathbb{E}_{\theta^*} (X_{\setminus r} X_r)$. The solution to (23), denoted as $\tilde{\theta}_{\setminus r}^*$, can be analytically obtained as $\tilde{\theta}_{\setminus r}^* = (Q_r^*)^{-1} b$. Next, we construct the full covariance matrix $C = \mathbb{E}_{\theta^*} (X X^T)$ of all spins X as follows

$$C = \begin{bmatrix} 1 & b^T \\ b & Q_r^* \end{bmatrix}, \quad (24)$$

where X_r is indexed as the first variable in C without loss of generality. From the block matrix inversion lemma, the inverse covariance matrix can be computed as

$$C^{-1} = \begin{bmatrix} F_{11}^{-1} & -F_{11}^{-1} (\tilde{\theta}_{\setminus r}^*)^T \\ -\tilde{\theta}_{\setminus r}^* F_{11}^{-1} & F_{22}^{-1} \end{bmatrix}, \quad (25)$$

where

$$F_{11} = 1 - b^T (Q_r^*)^{-1} b, \quad (26)$$

$$F_{22} = Q_r^* - b b^T. \quad (27)$$

On the other hand, for sparse tree-like graph in the paramagnetic phase, the inverse covariance matrix C^{-1} can be computed from the Hessian of the Gibbs free energy [Abbara et al., 2020, Nguyen and Berg, 2012, Ricci-Tersenghi, 2012]. Specifically, each element of the covariance matrix $C = \{C_{rt}\}_{r,t \in V}$ can be expressed as

$$C_{rt} = \mathbb{E}_{\theta^*} (x_r x_t) - \mathbb{E}_{\theta^*} (x_r) \mathbb{E}_{\theta^*} (x_t) = \frac{\partial^2 \log Z(\sigma)}{\partial \sigma_r \partial \sigma_t}, \quad (28)$$

where $Z(\sigma) = \sum_x \mathbb{P}_{\theta^*} (x) e^{\sum_{s \in V} \sigma_s x_s}$ with $\sigma = \{\sigma_s\}_{s \in V}$ and the assessment is carried out at $\sigma = 0$. In addition, for technical convenience we introduce the Gibbs free energy as

$$A(m) = \max_{\sigma} \{ \sigma^T m - \log Z(\sigma) \}. \quad (29)$$

The definition of (29) indicates that following two relations hold:

$$\frac{\partial m_r}{\partial \sigma_t} = \frac{\partial^2 \log Z(\sigma)}{\partial \sigma_r \partial \sigma_t} = C_{rt}, \quad (30)$$

$$\frac{\partial \sigma_r}{\partial m_t} = [C^{-1}]_{rt} = \frac{\partial^2 A(m)}{\partial m_r \partial m_t}, \quad (31)$$

where the evaluations are performed at $\sigma = 0$ and $m = \arg \min_m A(m)$ ($= 0$ under the paramagnetic assumption). Consequently, the inverse covariance matrix of a tree-like graph $G \in \mathcal{G}_{p,d}$ can be computed as [Abbara et al., 2020, Nguyen and Berg, 2012, Ricci-Tersenghi, 2012]

$$[C^{-1}]_{rt} = \left(\sum_{u \in \mathcal{N}(r)} \frac{1}{1 - \tanh^2(\theta_{ru}^*)} - d_r + 1 \right) \delta_{rt} - \frac{\tanh(\theta_{rt}^*)}{1 - \tanh^2(\theta_{rt}^*)} (1 - \delta_{rt}). \quad (32)$$

The two representations of C^{-1} in (25) and (32) are equivalent so that the corresponding elements should equal to each other. Thus, the following identities hold

$$\begin{cases} F_{11}^{-1} = \sum_{u \in \mathcal{N}(r)} \frac{1}{1 - \tanh^2(\theta_{ru}^*)} - d_r + 1, \\ \tilde{\theta}_{\setminus r}^* F_{11}^{-1} = \frac{\tanh(\theta_{\setminus r}^*)}{1 - \tanh^2(\theta_{\setminus r}^*)}, \end{cases} \quad (33)$$

where $\tanh(\cdot)$ is applied element-wise. From (33), we obtain (20), which is a rescaled version of the true couplings. In particular, for RR graphs with constant coupling $|\theta_{rt}^*| = \theta_0, \forall (r, t) \in E$ and $d_r = d$, substituting the results one can obtain (21), which completes the proof. \blacksquare

The result of Lemma 2 indicates that, under the assumption (A3), the solution $\tilde{\theta}_{\setminus r}^*$ to the zero-gradient condition $\mathbb{E}_{\theta^*}(\nabla \ell(\theta_{\setminus r}; \mathfrak{X}_1^n)) = 0$ with quadratic loss shares the same sign structure as the true parameter $\theta_{\setminus r}^*$, i.e., $\text{sign}(\tilde{\theta}_{\setminus r}^*) = \text{sign}(\theta_{\setminus r}^*)$. The minimum magnitude of the rescaled value $\tilde{\theta}_{rt}^*$ for $(r, t) \in E$ is denoted as

$$\tilde{\theta}_{\min}^* := \min_{(r,t) \in E} \tilde{\theta}_{rt}^*, \quad (34)$$

where $\tilde{\theta}_{rt}^*$ is defined in (20).

Subsequently, for any fixed $r \in V$, given $\tilde{\theta}_{\setminus r}^*$, we re-write the zero-subgradient condition (16) as follows

$$\nabla \ell(\hat{\theta}_{\setminus r}; \mathfrak{X}_1^n) - \nabla \ell(\tilde{\theta}_{\setminus r}^*; \mathfrak{X}_1^n) = W^n - \lambda_n \hat{z}, \quad (35)$$

where $W^n = -\nabla \ell(\tilde{\theta}_{\setminus r}^*; \mathfrak{X}_1^n)$ are evaluated at the rescaled $\tilde{\theta}_{\setminus r}^*$ in (20), as opposed to the true parameter $\theta_{\setminus r}^*$ [Ravikumar et al., 2010]. Using the mean-value theorem element-wise to (35), we obtain

$$\nabla^2 \ell(\tilde{\theta}_{\setminus r}^*; \mathfrak{X}_1^n) [\hat{\theta}_{\setminus r} - \tilde{\theta}_{\setminus r}^*] = W^n - \lambda_n \hat{z}. \quad (36)$$

In contrast to Ravikumar et al. [2010], the remainder term disappears due to the quadratic

quadratic loss (8). The s -th element of W^n , denoted as W_s^n , can be written as follows

$$W_s^n = \frac{1}{n} \sum_{i=1}^n Z_s^{(i)}, \quad \forall s \in V \setminus r, \quad (37)$$

$$Z_s^{(i)} := x_s^{(i)} \left(x_r^{(i)} - \sum_{t \in V \setminus r} \tilde{\theta}_{rt}^* x_t^{(i)} \right). \quad (38)$$

It can be seen that W^n has a quite different form from the result in Ravikumar et al. [2010]. The properties of the random variable $Z_s^{(i)}$ are shown in Lemma 3.

Lemma 3 *The random variable $Z_s^{(i)}$ defined in (38) has zero mean and bounded variance, i.e., $\mathbb{E}_{\theta^*} \left(Z_s^{(i)} \right) = 0$, $\text{Var} \left(Z_s^{(i)} \right) \leq 1$. Furthermore, $Z_s^{(i)}$ itself is bounded by $\left| Z_s^{(i)} \right| \leq d$.*

Proof First, $\mathbb{E}_{\theta^*} \left(Z_s^{(i)} \right) = 0$ can be readily obtained from Lemma 2. Thus, to prove $\text{Var} \left(Z_s^{(i)} \right) \leq 1$, it suffices to prove $\mathbb{E}_{\theta^*} \left(\left(Z_s^{(i)} \right)^2 \right) \leq 1$. To this end, we introduce an auxiliary function

$$f_1 \left(\theta_{\setminus r} \right) = \mathbb{E}_{\theta^*} \left(x_r^{(i)} - \sum_{t \in V \setminus r} \theta_t x_t^{(i)} \right)^2. \quad (39)$$

Thus we have $\mathbb{E}_{\theta^*} \left(\left(Z_s^{(i)} \right)^2 \right) = f_1 \left(\tilde{\theta}_{\setminus r}^* \right)$. The gradient vector can be computed as $\nabla f_1 \left(\theta_{\setminus r} \right) = 2\mathbb{E}_{\theta^*} \left(\nabla \ell \left(\theta_{\setminus r}; \mathfrak{X}_1^n \right) \right)$. Since $\mathbb{E}_{\theta^*} \left(\nabla \ell \left(\tilde{\theta}_{\setminus r}^*; \mathfrak{X}_1^n \right) \right) = 0$ as shown in Lemma 2, we have $\nabla f_1 \left(\tilde{\theta}_{\setminus r}^* \right) = 0$. Moreover, since $\nabla^2 f_1 \left(\theta_{\setminus r} \right) = 2\mathbb{E}_{\theta^*} \left(X_{\setminus r} X_r \right) \succ 0$, we can conclude that $f_1 \left(\theta_{\setminus r} \right)$ reaches its minimum at $\theta_{\setminus r} = \tilde{\theta}_{\setminus r}^*$. As a result, we have

$$\begin{aligned} \mathbb{E}_{\theta^*} \left(\left(Z_s^{(i)} \right)^2 \right) &= f_1 \left(\theta_{\setminus r} = \tilde{\theta}_{\setminus r}^* \right) \\ &\leq f_1 \left(\theta_{\setminus r} = 0 \right) \\ &= \mathbb{E}_{\theta^*} \left(x_r^{(i)} \right)^2 \\ &= 1, \end{aligned}$$

where in the last line the fact that $x_r^{(i)} \in \{-1, +1\}$, $\forall r \in V$ is used. Therefore, we obtain $\text{Var} \left(Z_s^{(i)} \right) \leq 1$.

Finally, recalling the result (20), we have

$$\begin{aligned}
& \left(\sum_{u \in \mathcal{N}(r)} \frac{1}{1 - \tanh^2(\theta_{ru}^*)} - d_r + 1 \right) \sum_{t \in V \setminus r} |\tilde{\theta}_{rt}^*| \\
&= \sum_{t \in \mathcal{N}(r)} \frac{|\tanh(\theta_{rt}^*)|}{1 - \tanh^2(\theta_{rt}^*)} \\
&= \sum_{t \in \mathcal{N}(r)} \frac{|\tanh(\theta_{rt}^*)| + 1 - \tanh^2(\theta_{rt}^*) + \tanh^2(\theta_{rt}^*) - 1}{1 - \tanh^2(\theta_{rt}^*)} \\
&= -d_r + \sum_{t \in \mathcal{N}(r)} \frac{|\tanh(\theta_{rt}^*)| + 1 - \tanh^2(\theta_{rt}^*)}{1 - \tanh^2(\theta_{rt}^*)}, \tag{40}
\end{aligned}$$

To proceed, consider an auxiliary function $f_2(x) = x + 1 - x^2, 0 \leq x \leq 1$. Then it can be proved that $1 \leq f_2(x) \leq \frac{5}{4}$, so that from (40), we have

$$\sum_{t \in V \setminus r} |\tilde{\theta}_{rt}^*| \leq \frac{-d_r + \frac{5}{4} \sum_{u \in \mathcal{N}(r)} \frac{1}{1 - \tanh^2(\theta_{ru}^*)}}{\sum_{u \in \mathcal{N}(r)} \frac{1}{1 - \tanh^2(\theta_{ru}^*)} - d_r + 1}. \tag{41}$$

It can be easily checked that $\sum_{u \in \mathcal{N}(r)} \frac{1}{1 - \tanh^2(\theta_{ru}^*)} \in [d_r, \infty)$. We introduce another auxiliary function

$$f_3(x) = \frac{-d_r + \frac{5}{4}x}{x - d_r + 1}, x \in [d_r, \infty). \tag{42}$$

The first-order derivative of $f_3(x)$ can be easily computed as

$$f_3'(x) = \frac{5 - d_r}{4(x - d_r + 1)^2}. \tag{43}$$

As a result, $f_3'(x) > 0$ when $d_r < 5$ and $f_3'(x) < 0$ when $d_r > 5$. Consequently,

$$\max_{x \in [d_r, \infty)} f_3(x) = \begin{cases} \frac{5}{4} & d_r \leq 5 \\ \frac{d_r}{4} & d_r > 5 \end{cases} \tag{44}$$

Finally, combining the above results together yields

$$|Z_s^{(i)}| \leq \max \left\{ \frac{9}{4}, \frac{4 + d_r}{4} \right\} < d_r, \forall d_r \geq 3. \tag{45}$$

By definition, there is $d_r \leq d$ so that $|Z_s^{(i)}| \leq d$, which completes the proof. \blacksquare

Using the results in Lemma 3, we can obtain the behavior of $\|W^n\|_\infty$, as shown in the following lemma.

Lemma 4 *For the specified mutual incoherence parameter $\alpha \in (0, 1]$, if $n \geq (c + 1) d^2 \log p$ for some constant $c > 0$ and $\lambda_n \geq \frac{4\sqrt{c+1}(2-\alpha)}{\alpha} \sqrt{\frac{\log p}{n}}$, then*

$$\mathbb{P}\left(\frac{2-\alpha}{\lambda_n} \|W^n\|_\infty \geq \frac{\alpha}{2}\right) \leq 2 \exp(-c \log p), \quad (46)$$

which converges to zero at rate $\exp(-c \log p)$ as $p \rightarrow +\infty$.

Proof According to Lemma 3, applying the Bernstein's inequality [Vershynin, 2018], $\forall \eta > 0$ we have

$$\mathbb{P}(|W_s^n| > \eta) \leq 2 \exp\left(-\frac{\frac{1}{2}\eta^2 n}{1 + \frac{1}{3}d\eta}\right). \quad (47)$$

Similar to Vuffray et al. [2016], inverting the following relation

$$\xi = \frac{\frac{1}{2}\eta^2 n}{1 + \frac{1}{3}d\eta}, \quad (48)$$

and substituting the result in (47) yields

$$\mathbb{P}\left(|W_s^n| > \frac{1}{3}\left(u + \sqrt{u^2 + 18\frac{u}{d}}\right)\right) \leq 2 \exp(-\xi), \quad (49)$$

where $u = \frac{\xi}{n}d$. Suppose that $n \geq \xi d^2$, then $u^2 = \frac{\xi^2}{n^2}d^2 \leq \frac{\xi}{n}$ while $\frac{u}{d} = \frac{\xi}{n}$. Consequently, we have

$$\begin{aligned} \frac{1}{3}\left(u + \sqrt{u^2 + 18\frac{u}{d}}\right) &\leq \frac{1}{3}\left(\sqrt{\frac{\xi}{n}} + \sqrt{\frac{\xi}{n} + 18\frac{\xi}{n}}\right) \\ &\leq \frac{1}{3}\left(\sqrt{\frac{\xi}{n}} + \sqrt{\frac{\xi}{n}}\sqrt{25}\right) \\ &= 2\sqrt{\frac{\xi}{n}}, \end{aligned}$$

where a relaxed result is obtained. Subsequently, we obtain an expression which is independent of d :

$$\mathbb{P}\left(|W_s^n| > 2\sqrt{\frac{\xi}{n}}\right) \leq 2 \exp(-\xi). \quad (50)$$

Setting $\xi = (c + 1) \log p$, then if $\lambda_n \geq \frac{4(2-\alpha)\sqrt{c+1}}{\alpha} \sqrt{\frac{\log p}{n}}$, we have $\frac{\alpha\lambda_n}{2(2-\alpha)} \geq 2\sqrt{\frac{\xi}{n}}$ so that

$$\mathbb{P}\left(\frac{2-\alpha}{\lambda_n} |W_s^n| > \frac{\alpha}{2}\right) \leq \mathbb{P}\left(|W_s^n| > 2\sqrt{\frac{\xi}{n}}\right) \leq 2 \exp(-(c+1) \log p). \quad (51)$$

Then, by using a union bound we have

$$\mathbb{P}\left(\frac{2-\alpha}{\lambda_n} \|W^n\|_\infty \geq \frac{\alpha}{2}\right) \leq 2 \exp(-c \log p). \quad (52)$$

As a result, when $n \geq (c+1)d^2 \log p$, as long as $\lambda_n \geq \frac{4\sqrt{c+1}(2-\alpha)}{\alpha} \sqrt{\frac{\log p}{n}}$, it is guaranteed that $\mathbb{P}\left(\frac{2-\alpha}{\lambda_n} \|W^n\|_\infty \geq \frac{\alpha}{2}\right) \rightarrow 0$ at rate $\exp(-c \log p)$ for some constant $c > 0$, which completes the proof. \blacksquare

Moreover, it can be also proved that the sub-vector $\hat{\theta}_S$ is an ℓ_2 -consistent estimate of the rescaled sub-vector $\tilde{\theta}_S^*$, as opposed to the original sub-vector θ_S^* in Ravikumar et al. [2010], as stated in the following lemma:

Lemma 5 (*ℓ_2 -consistency of the primal sub-vector*). *If $\|W^n\|_\infty \leq \frac{\lambda_n}{2}$, then there is*

$$\|\hat{\theta}_S - \tilde{\theta}_S^*\|_2 \leq \frac{3}{C_{\min}} \lambda_n \sqrt{d}. \quad (53)$$

Proof Using the method in Rothman et al. [2008], here the proof follows Ravikumar et al. [2010] but with some modifications. First, define a function $\mathbb{R}^d \rightarrow \mathbb{R}$ as follows [Rothman et al., 2008]

$$G(u_S) := \ell(\tilde{\theta}_S^* + u_S; \mathfrak{X}_1^n) - \ell(\tilde{\theta}_S^*; \mathfrak{X}_1^n) + \lambda_n \left(\|\tilde{\theta}_S^* + u_S\|_1 - \|\tilde{\theta}_S^*\|_1 \right). \quad (54)$$

Note that G is a convex function w.r.t. u_S . Then $\hat{u}_S = \hat{\theta}_S - \tilde{\theta}_S^*$ minimizes G according to the definition in (7). Moreover, it is easily seen that $G(0) = 0$ so that $G(\hat{u}_S) \leq 0$. As described in Ravikumar et al. [2010], if we can show that there exists some radius $B > 0$ and any $u_S \in \mathbb{R}^d$ with $\|u_S\|_2 = B$ satisfies $G(u_S) > 0$, then we can claim that $\|\hat{u}_S\|_2 \leq B$ since otherwise one can always, by appropriately choosing $t \in (0, 1]$, find a convex combination $t\hat{u}_S + (1-t)0$ which lies on the boundary of the ball with radius B and thus $G(t\hat{u}_S + (1-t)0) \leq 0$, leading to contradiction. Consequently, it suffices to establish the strict positivity of G on the boundary of a ball with radius $B = M\lambda_n\sqrt{d}$, where $M > 0$ is one parameter to choose later.

Specifically, let $u_S \in \mathbb{R}^d$ be an arbitrary vector with $\|u_S\|_2 = B$. Expanding the

quadratic form $\ell\left(\tilde{\theta}_S^* + u_S; \mathfrak{X}_1^n\right)$, we have

$$G(u_S) = -(W_S^n)^T u_S + u_S^T Q_S^n u_S + \lambda_n \left(\left\| \tilde{\theta}_S^* + u_S \right\|_1 - \left\| \tilde{\theta}_S^* \right\|_1 \right), \quad (55)$$

where W_S^n is the sub-vector of $W^n = -\nabla \ell\left(\tilde{\theta}^*; \mathfrak{X}_1^n\right)$, and Q_S^n is the sub-matrix of the sample covariance matrix $Q^n = \frac{1}{n} \sum_i X_{\setminus r}^{(i)} \left(X_{\setminus r}^{(i)}\right)^T$. The expression (55) is simpler than the counterpart in Ravikumar et al. [2010] which is obtained from the Taylor series expansion of the non-quadratic loss function and thus its quadratic term is dependent on θ . To proceed, we investigate the bounds of the three terms in the right hand side (RHS) of (55), respectively.

Since $\|u_S\|_1 \leq \sqrt{d} \|u_S\|_2$ and $\|W_S^n\|_\infty \leq \frac{\lambda_n}{2}$, the first term is bounded as

$$\left| -(W_S^n)^T u_S \right| \leq \|W_S^n\|_\infty \|u_S\|_1 \leq \|W_S^n\|_\infty \sqrt{d} \|u_S\|_2 \leq \left(\lambda_n \sqrt{d} \right)^2 \frac{M}{2}. \quad (56)$$

The third term is bounded as

$$\lambda_n \left(\left\| \tilde{\theta}_S^* + u_S \right\|_1 - \left\| \tilde{\theta}_S^* \right\|_1 \right) \geq -\lambda_n \|u_S\|_1 \geq -\lambda_n \sqrt{d} \|u_S\|_2 = -M \left(\lambda_n \sqrt{d} \right)^2. \quad (57)$$

The remaining middle Hessian term in RHS of (55) is, different from Ravikumar et al. [2010], quite simple due to the quadratic loss function:

$$\begin{aligned} u_S^T Q_S^n u_S &\geq \|u_S\|_2^2 \Lambda_{\min} \left(\frac{1}{n} \sum_i X_S^{(i)} \left(X_S^{(i)}\right)^T \right) \\ &= \|u_S\|_2^2 \Lambda_{\min} (Q_{SS}^*) \\ &\geq C_{\min} M^2 \left(\lambda_n \sqrt{d} \right)^2, \end{aligned} \quad (58)$$

where the last inequality comes from the dependency condition $\Lambda_{\min} (Q_{SS}^*) \geq C_{\min}$ in (10). In contrast to Ravikumar et al. [2010], there is no need to control the additional spectral norm.

Combining the three bounds (56) - (58) together with (55), we obtain that

$$G(u_S) \geq \left(\lambda_n \sqrt{d} \right)^2 \left\{ -\frac{M}{2} + C_{\min} M^2 - M \right\}. \quad (59)$$

It can be easily verified from (59) that $G(u_S)$ is strictly positive when we choose $M = \frac{3}{C_{\min}}$. Consequently, as long as $\|W^n\|_\infty \leq \frac{\lambda_n}{2}$, we are guaranteed that $\|\hat{u}_S\|_2 \leq M \lambda_n \sqrt{d} = \frac{3\lambda_n \sqrt{d}}{C_{\min}}$, which completes the proof. \blacksquare

4.3 Proof of Theorem 1

From Lemma 4, when $n \geq (c+1)d^2 \log p$, if the regularization parameter is chosen to satisfy $\lambda_n \geq \frac{4\sqrt{c+1}(2-\alpha)}{\alpha} \sqrt{\frac{\log p}{n}}$, it is guaranteed that with probability greater than $1 - 2 \exp(-c \log p)$ ($\rightarrow 1$ in the high dimensional setting for $p \rightarrow \infty$), we have

$$\|W^n\|_\infty \leq \frac{\alpha}{2-\alpha} \frac{\lambda_n}{2} \leq \frac{\lambda_n}{2}, \quad (60)$$

where $0 < \alpha \leq 1$ is used in the last inequality, so that the condition in Lemma 5 is also satisfied. The zero-subgradient condition (36) can be equivalently re-written as follows

$$\begin{cases} Q_{S^c S}^n (\hat{\theta}_S - \tilde{\theta}_S^*) = W_{S^c}^n - \lambda_n \hat{z}_{S^c}, \\ Q_{SS}^n (\hat{\theta}_S - \tilde{\theta}_S^*) = W_S^n - \lambda_n \hat{z}_S, \end{cases} \quad (61)$$

where we have used the fact that $\hat{\theta}_{S^c} = 0$ from the primal-dual construction. After some simple algebra and rearrangement as Ravikumar et al. [2010], we obtain

$$W_{S^c}^n - Q_{S^c S}^n (Q_{SS}^n)^{-1} W_S^n + \lambda_n Q_{S^c S}^n (Q_{SS}^n)^{-1} \hat{z}_S = \lambda_n \hat{z}_{S^c}. \quad (62)$$

For strict dual feasibility, from (62), using the triangle inequality and the mutual incoherence bound, we have

$$\begin{aligned} \|\hat{z}_{S^c}\|_\infty &\leq \|Q_{S^c S}^* (Q_{SS}^*)^{-1}\|_\infty \left[\frac{\|W_S^n\|_\infty}{\lambda_n} + 1 \right] + \frac{\|W_{S^c}^n\|_\infty}{\lambda_n} \\ &\leq (1-\alpha) + (2-\alpha) \frac{\|W^n\|_\infty}{\lambda_n} \\ &\leq (1-\alpha) + (2-\alpha) \frac{1}{2-\alpha} \frac{\alpha}{2} \\ &= 1 - \frac{\alpha}{2} < 1, \end{aligned} \quad (63)$$

with probability converging to one. For correct sign recovery, it suffices to show that $\|\hat{\theta}_S - \tilde{\theta}_S^*\|_\infty \leq \frac{\tilde{\theta}_{\min}^*}{2}$. From Lemma 5 (since (60) holds), we have

$$\begin{aligned} \frac{2}{\theta_{\min}^*} \|\hat{\theta}_S - \tilde{\theta}_S^*\|_\infty &\leq \frac{2}{\theta_{\min}^*} \|\hat{\theta}_S - \tilde{\theta}_S^*\|_2 \\ &\leq \frac{2}{\tilde{\theta}_{\min}^*} \frac{3}{C_{\min}} \lambda_n \sqrt{d} \end{aligned}$$

$$= \frac{6}{\tilde{\theta}_{\min}^* C_{\min}} \lambda_n \sqrt{d}. \quad (64)$$

As a result, if $\tilde{\theta}_{\min}^* \geq \frac{6\lambda_n \sqrt{d}}{C_{\min}}$, or equivalently $\lambda_n \leq \frac{\tilde{\theta}_{\min}^* C_{\min}}{6\sqrt{d}}$, the condition $\|\hat{\theta}_S - \tilde{\theta}_S^*\|_{\infty} \leq \frac{\tilde{\theta}_{\min}^*}{2}$ holds.

4.4 Proof of Theorem 2

Given Theorem 1, the proof of Theorem 2 is straightforward following the same line in Ravikumar et al. [2010]. For completeness, we restate the associated results in Ravikumar et al. [2010] without giving the proofs. In the case of quadratic loss, only the covariance matrix is concerned and thus we only need to focus on the covariance matrix.

Lemma 6 (Lemma 5 in Ravikumar et al. [2010]) Denote $Q^n := \frac{1}{n} \sum_i X_{\setminus r}^{(i)} \left(X_{\setminus r}^{(i)} \right)^T$. If the dependency condition (A1) holds for the population covariance $Q^* := \mathbb{E}_{\theta^*} \left\{ X_{\setminus r} X_{\setminus r}^T \right\}$, then for any $\delta > 0$, there are some constants A and B

$$\mathbb{P} \left(\Lambda_{\max} \left(\frac{1}{n} \sum_i X_{\setminus r}^{(i)} \left(X_{\setminus r}^{(i)} \right)^T \right) \geq D_{\max} + \delta \right) \leq 2 \exp \left(-A \frac{\delta^2 n}{d^2} + B \log d \right), \quad (65)$$

$$\mathbb{P} \left(\Lambda_{\min} (Q_{SS}^n) \leq C_{\min} - \delta \right) \leq 2 \exp \left(-A \frac{\delta^2 n}{d^2} + B \log d \right). \quad (66)$$

The following lemma is the analog for the incoherence condition (A2), showing that the scaling of (n, p, d) guarantees that the population incoherence implies sample incoherence.

Lemma 7 (Lemma 6 in Ravikumar et al. [2010]) If the incoherence condition (11) holds for the population covariance $Q^* := \mathbb{E}_{\theta^*} \left\{ X_{\setminus r} X_{\setminus r}^T \right\}$, then the sample covariance matrix satisfies an analogous version, with high probability in the sense that

$$\mathbb{P} \left(\left\| Q_{ScS}^n (Q_{SS}^n)^{-1} \right\|_{\infty} \geq 1 - \frac{\alpha}{2} \right) \leq 2 \exp \left(-K \frac{n}{d^3} + \log p \right), \quad (67)$$

where $K > 0$ is some constant.

Consequently, if the population covariance matrix $Q^* := \mathbb{E}_{\theta^*} \left\{ X_{\setminus r} X_{\setminus r}^T \right\}$ satisfies the dependency condition (A1) and incoherence condition (A2), then analogous bounds hold for the sample covariance matrix $Q^n := \frac{1}{n} \sum_i X_{\setminus r}^{(i)} \left(X_{\setminus r}^{(i)} \right)^T$ and thus we can obtain Theorem 2 by combining Theorem 1 with Lemma 6 and Lemma 7 as Ravikumar et al. [2010].

5 Experimental Results

In this section we conduct simulations to verify our theoretical analysis. For tree-like graphs, both RR and star-shaped graphs are evaluated, representing the bounded node degree case and unbounded node degree case, respectively. In addition, as an example of graphs with many loops, we also evaluate the case of 4 nearest-neighbor square lattice (grid) graphs with periodic boundary condition.

The experimental procedures are as follows. First, a graph $G = (V, E) \in \mathcal{G}_{p,d}$ is generated and the Ising model is defined on it. Then, the spin snapshots are obtained using Monte-Carlo sampling, yielding the dataset \mathfrak{X}_1^n . The regularization parameter is set to be a constant factor of $\sqrt{\frac{\log p}{n}}$. For any graph, we performed simulations using the neighborhood-based Lasso estimator (7) for $\forall r \in V$ and then the associated signed neighborhood $\hat{\mathcal{N}}_{\pm}(r)$ is estimated as (6). Similar to Ravikumar et al. [2010], the sample size n scaling is set to be proportional to $d \log p$. For comparison, the results of the ℓ_1 -LogR estimator [Ravikumar et al., 2010] are also shown. The results are averaged over 200 trials in all cases.

For RR graph, we consider the case with mixed couplings $\theta_{rt}^* = \pm 0.4$ and constant degree $d = 3$. Fig. 1 shows the success probability versus the control parameter $\beta = \frac{n}{10d \log p}$ for 3-nearest neighbor RR graph for different model sizes $p = 200, 400, 800$. It can be seen in Fig. 1 that using the Lasso estimator, despite different values of n, p that underlie each curve, all the three curves line up with each other well, showing that for a graph with fixed degree d , the ratio $n/\log p$ controls the success or failure of the Ising model selection. The behavior of the Lasso estimator is about the same as the ℓ_1 -LogR estimator.

In the case of star-shaped graph, the maximum degree d is unbounded and it grows as the dimension p grows. We consider two kinds of star-shaped graphs as Ravikumar et al. [2010] by designating one node as the hub and connecting it to $d < (p - 1)$ of its neighbors. Specifically, for linear sparsity, it is assumed that $d = \lceil 0.1p \rceil$ while for logarithmic sparsity, we assume $d = \lceil \log p \rceil$. We use positive couplings and set the active couplings to be $\theta_{rt}^* = \frac{1.2}{\sqrt{d}}$ for all $(r, t) \in E$ as Ravikumar et al. [2010]. Three different model dimension $p = 64, 100, 225$ are evaluated. Fig. 2 and Fig. 3 show the success probability versus the control parameter β for star-shaped graphs with linear sparsity and logarithmic sparsity, respectively. As with the RR graph in Fig. 1, the results for growing degree of star-shaped graphs also line up with each other well, which is consistent with our theoretical analysis.

Finally, the results of 4-nearest neighbor grid graph with positive couplings $\theta_{rt}^* = 0.2$ for all $(r, t) \in E$ are shown in Fig. 4. It can be seen that, even in the case of graph with many loops, the Lasso estimator also behaves similarly to the ℓ_1 -LogR estimator.

6 Conclusion

In this paper we have rigorously demonstrated that using the neighborhood-based Lasso, one can obtain consistent model selection for Ising models on any tree-like graph in the

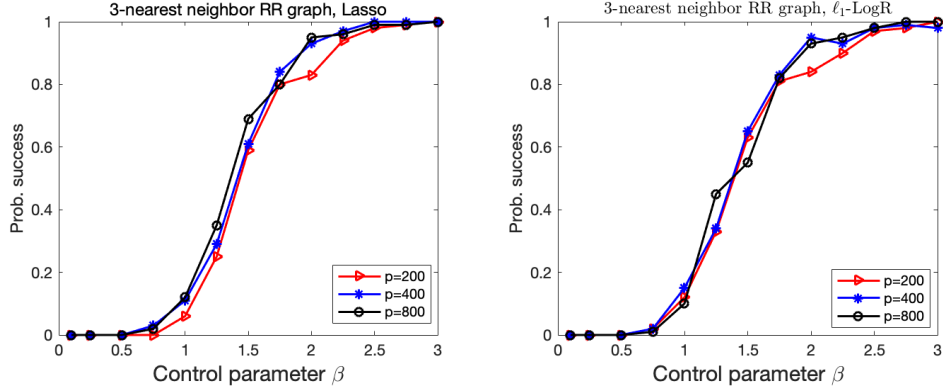


Figure 1: Plots of success probability $\mathbb{P}\left(\hat{\mathcal{N}}_{\pm}(r) = \mathcal{N}_{\pm}(r), \forall r \in V\right)$ versus the control parameter $\beta = \frac{n}{10d \log p}$ for Ising models on 3-nearest neighbor RR graph with $d = 3$ and mixed couplings $\theta_{rt}^* = \pm 0.4$ for all $(r, t) \in E$. Left: Lasso; Right: ℓ_1 -LogR.

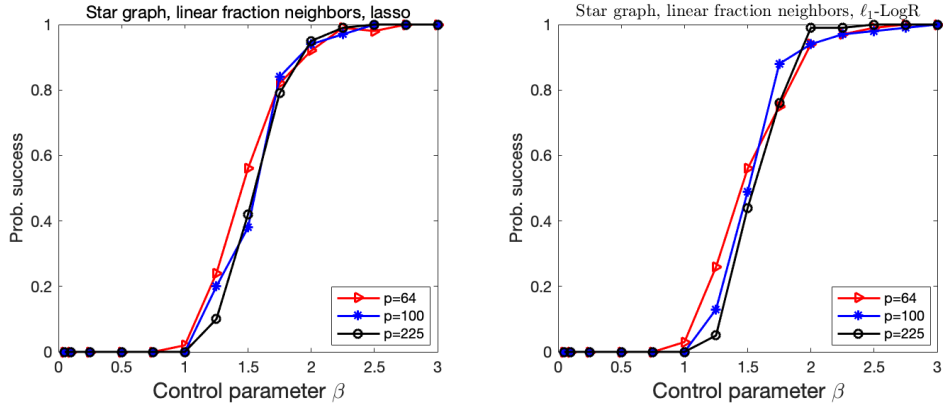


Figure 2: Plots of success probability $\mathbb{P}\left(\hat{\mathcal{N}}_{\pm}(r) = \mathcal{N}_{\pm}(r), \forall r \in V\right)$ versus the control parameter $\beta = \frac{n}{10d \log p}$ for Ising models on star-shaped graphs for attractive couplings $\theta_{rt}^* = \frac{1.2}{\sqrt{d}}$ for all $(r, t) \in E$ with linear growth in degrees, i.e., $d = \lceil 0.1p \rceil$. Left: Lasso; Right: ℓ_1 -LogR.

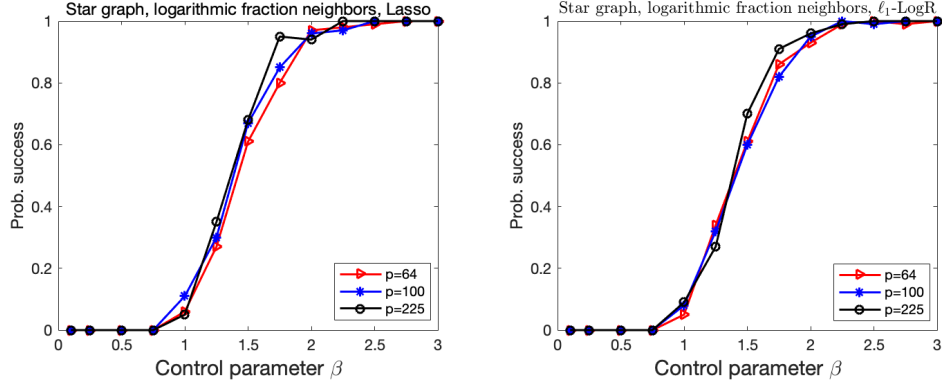


Figure 3: Plots of success probability $\mathbb{P}\left(\hat{\mathcal{N}}_{\pm}(r) = \mathcal{N}_{\pm}(r), \forall r \in V\right)$ versus the control parameter $\beta = \frac{n}{10d \log p}$ for Ising models on star-shaped graphs for attractive couplings $\theta_{rt}^* = \frac{1.2}{\sqrt{d}}$ for all $(r, t) \in E$ with logarithmic growth in degrees, i.e., $d = \lceil \log p \rceil$. Left: Lasso; Right: ℓ_1 -LogR.

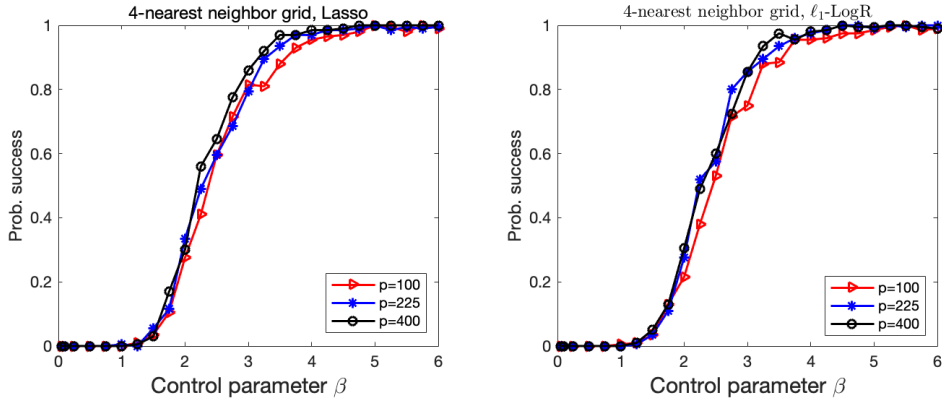


Figure 4: Plots of success probability $\mathbb{P}\left(\hat{\mathcal{N}}_{\pm}(r) = \mathcal{N}_{\pm}(r), \forall r \in V\right)$ versus the control parameter $\beta = \frac{n}{15d \log p}$ for Ising models on 4-nearest neighbor grid graph with $d = 4$ and positive couplings $\theta_{rt}^* = 0.2$ for all $(r, t) \in E$.

paramagnetic phase. The high-dimensional regime is applicable where both the number of nodes p and maximum node degree d grow as a function of the samples n . Remarkably, the obtained sample complexity for consistent model selection with Lasso has the same scaling as that of ℓ_1 -LogR [Ravikumar et al., 2010]. Experimental results on RR, star-shaped (both linear and logarithmic fraction neighbors), and even grid graphs with many loops are consistent with the theoretical predictions.

As future work, it is interesting to clarify the class of loss functions exhibiting the model consistency despite the model misspecification. For this purpose, an important quantity manifested from the current study is the estimator $\tilde{\theta}_{\setminus r}$ derived from the zero-gradient condition of the expected loss; showing its model consistency is the largest difference in the proof steps from Ravikumar et al. [2010]. In the present case, the loss is quadratic and it is not difficult to show its model consistency, but in the general case it would become a nontrivial task. Nevertheless, in Abbara et al. [2020] it has been shown by employing the tree structure of the generative Ising model that $\tilde{\theta}_{\setminus r}$ is model consistent for a wide class of loss functions corresponding to the single index model with the argument $\sum_{t(\neq r)} \theta_{rt}^* x_r x_t$. Their “proof” is using the replica method and thus is not rigorous. Moreover, it lacks a detailed consideration about the fluctuation of the estimator $\hat{\theta}_{\setminus r}$ from $\tilde{\theta}_{\setminus r}$. Filling these gaps and clarifying the “precise class” of model-consistent loss functions will be an interesting generalization of the present work. Relaxing the assumption (A3), especially the tree structure assumption of the generative model, is also important.

Another interesting future work is to clarify the performance of Lasso or related estimators in the low temperature phases involving spontaneous symmetry breaking. It is shown in Lokhov et al. [2018] that even in the low temperature region the graph reconstruction is possible with a reasonable sample complexity by using the interaction screening estimator, if the i.i.d.ness of the samples holds. However, it is not easy to perform correct sampling after phase transitions, and hence the generated samples tend to be biased and be not i.i.d.. We have conducted some numerical experiments in such situations and found that even with biased samples the graph reconstruction seems to be possible. Besides, it is very recently reported that a significant reduction of the sample complexity is possible by using non i.i.d. samples [Dutt et al., 2021]. Building a theory supporting this finding is an interesting direction and some theoretical efforts are currently undergoing.

Acknowledgement

We are thankful to Martin J. Wainwright and Pradeep Ravikumar for kindly providing their experimental settings of star-shaped graphs.

Appendices

Appendix A A lower bound of $\tilde{\theta}_{\min}^*$

From the result (20) in Lemma 2, it is easy to obtain that $\forall (r, t) \in E$, we have

$$\begin{aligned}
|\tilde{\theta}_{rt}^*| &= \frac{1}{1 - d_r + \sum_{u \in \mathcal{N}(r)} \frac{1}{1 - \tanh^2(\theta_{ru}^*)}} \frac{|\tanh(\theta_{rt}^*)|}{1 - \tanh^2(\theta_{rt}^*)} \\
&\geq \frac{1}{1 - d_r + \frac{d_r}{1 - \tanh^2(\theta_{\max}^*)}} \frac{|\tanh(\theta_{\min}^*)|}{1 - \tanh^2(\theta_{\min}^*)} \\
&\geq \frac{1}{1 - d + \frac{d}{1 - \tanh^2(\theta_{\max}^*)}} \frac{|\tanh(\theta_{\min}^*)|}{1 - \tanh^2(\theta_{\min}^*)} \\
&= \frac{1 - \tanh^2(\theta_{\max}^*)}{1 + (d - 1) \tanh^2(\theta_{\max}^*)} \frac{\tanh(\theta_{\min}^*)}{1 - \tanh^2(\theta_{\min}^*)}. \tag{68}
\end{aligned}$$

As a result, $\tilde{\theta}_{\min}^* \geq \frac{1 - \tanh^2(\theta_{\max}^*)}{1 + (d - 1) \tanh^2(\theta_{\max}^*)} \frac{\tanh(\theta_{\min}^*)}{1 - \tanh^2(\theta_{\min}^*)}$.

Appendix B Proof of Proposition 1

Before the proof, we first introduce the following Lemma.

Lemma 8 *For a RR graph with uniform coupling strength θ_0 and constant node degree d . Under the paramagnetic assumption, the covariance between x_r and x_t can be calculated to be $\mathbb{E}_{\theta^*} \{x_r x_t\} - \mathbb{E}_{\theta^*} \{x_r\} \mathbb{E}_{\theta^*} \{x_t\} = \tanh^l(\theta_0)$, where l is the distance between node s and node t in the graph.*

Proof The Ising model on a RR graph can be analytically solvable by Bethe approximation. Specifically, the corresponding belief propagation (BP) equation can be written as follows [Mezard and Montanari, 2009]

$$m_{r \rightarrow t} = \tanh \left(\sum_{k \in \mathcal{N}(r) \setminus t} \tanh^{-1}(\tanh(\theta_0) m_{k \rightarrow r}) \right). \tag{69}$$

where $m_{r \rightarrow t}$ is the message from node r to node t . The spontaneous magnetization for the node $r \in V$ is assessed as

$$m_r = \tanh \left(\sum_{t \in \mathcal{N}(r)} \tanh^{-1}(\tanh(\theta_0) m_{t \rightarrow r}) \right). \tag{70}$$

Due to the uniformity of RR graphs, these equations are reduced to

$$m_c = \tanh \left((d-1) \tanh^{-1} (\tanh(\theta_0) m_c) \right), \quad (71)$$

$$m = \tanh \left(d \tanh^{-1} (\tanh(\theta_0) m_c) \right), \quad (72)$$

where we set $m_{r \rightarrow t} := m_c$ and $m_r := m$ for all directed edges $r \rightarrow t$ and all nodes $r \in V$.

Suppose that $x = (x_r)_{r=1}^p$ is subject to a Hamiltonian $H(x) = -\sum_{s \neq t} \theta_{rt}^* x_r x_t$. For this, we define the Helmholtz free energy as

$$F(\xi) = -\ln \left(\sum_x \exp \left(-H(x) + \sum_{r=1}^p \xi_r x_r \right) \right). \quad (73)$$

Using $F(\xi)$, one can evaluate the expectation of x as

$$m_r := \mathbb{E}_{\theta^*} \{x_r\} = - \left. \frac{\partial F(\xi)}{\partial \xi_r} \right|_{\xi=0} = \frac{\sum_x x_r \exp(-H(x))}{\sum_x \exp(-H(x))}. \quad (74)$$

In addition, the covariance of x_r and x_t can be computed as

$$\begin{aligned} & \mathbb{E}_{\theta^*} \{x_r x_t\} - \mathbb{E}_{\theta^*} \{x_r\} \mathbb{E}_{\theta^*} \{x_t\} \\ &= \left. \frac{\partial \mathbb{E}_{\theta^*} \{x_r\}}{\partial \xi_t} \right|_{\xi=0} \\ &= \frac{\sum_x x_r x_t \exp(-H(x))}{\sum_x \exp(-H(x))} - \frac{\sum_x x_r \exp(-H(x))}{\sum_x \exp(-H(x))} \cdot \frac{\sum_x x_t \exp(-H(x))}{\sum_x \exp(-H(x))}, \end{aligned} \quad (75)$$

$$(76)$$

where the last equation is termed the *linear response relation*.

Suppose that node r is placed at the distance of l from node t . A remarkable property of tree graphs, including RR graph, is that a unique path is defined between two arbitrary nodes. This indicates that the linear response relation (76) can be evaluated by the chain rule of partial derivative using messages of belief propagation as

$$\mathbb{E}_{\theta^*} \{x_r x_t\} - \mathbb{E}_{\theta^*} \{x_r\} \mathbb{E}_{\theta^*} \{x_t\} = \left. \frac{\partial m_r}{\partial \xi_t} \right|_{\xi=0} = (1 - m^2) \left(\frac{\tanh(\theta_0) (1 - m_c^2)}{1 - \tanh^2(\theta_0) m_c^2} \right)^l. \quad (77)$$

Under the paramagnetic assumption, there are $m = 0$ and $m_c = 0$. As a result, one obtain

$$\mathbb{E}_{\theta^*} \{x_r x_t\} - \mathbb{E}_{\theta^*} \{x_r\} \mathbb{E}_{\theta^*} \{x_t\} = \tanh^l(\theta_0). \quad (78)$$

■

Now we are ready for the proof. First, we consider the *dependency condition*. In the case of RR graph, the distances between any two different nodes in $S := \{(r, t) \mid t \in \mathcal{N}(r)\}$ are

2. Consequently, according to Lemma 8, all the off-diagonal elements in sub-matrix Q_{SS}^* equal to $\tanh^2 \theta_0$ and all the diagonal elements equal to 1, i.e.,

$$Q_{SS}^* = \begin{bmatrix} 1 & \tanh^2 \theta_0 & \tanh^2 \theta_0 & \cdots & \tanh^2 \theta_0 \\ \tanh^2 \theta_0 & 1 & \tanh^2 \theta_0 & \vdots & \tanh^2 \theta_0 \\ \tanh^2 \theta_0 & \tanh^2 \theta_0 & \ddots & \tanh^2 \theta_0 & \vdots \\ \vdots & \cdots & \tanh^2 \theta_0 & 1 & \tanh^2 \theta_0 \\ \tanh^2 \theta_0 & \tanh^2 \theta_0 & \cdots & \tanh^2 \theta_0 & 1 \end{bmatrix}_{d \times d}. \quad (79)$$

It can be analytically computed that Q_{SS}^* has two different eigenvalues: one is $1 + (d - 1) \tanh^2 \theta_0$ and the other is $1 - \tanh^2 \theta_0$ with multiplicity $(d - 1)$. Consequently, Q_{SS}^* has bounded eigenvalue and we explicitly obtain the result of C_{\min} as

$$\Lambda_{\min}(Q_{SS}^*) = 1 - \tanh^2 \theta_0 := C_{\min}. \quad (80)$$

Then, we prove that the *incoherence condition* also satisfies. From (79), the inverse matrix $(Q_{SS}^*)^{-1}$ can be analytically computed as

$$(Q_{SS}^*)^{-1} = \begin{bmatrix} a & b & b & \cdots & b \\ b & a & b & \vdots & b \\ b & b & \ddots & b & \vdots \\ \vdots & \cdots & b & a & b \\ b & b & \cdots & b & a \end{bmatrix}_{d \times d}, \quad (81)$$

where

$$a = \frac{1 + (d - 2) \tanh^2 \theta_0}{(1 - \tanh^2 \theta_0) (1 + (d - 1) \tanh^2 \theta_0)}, \quad (82)$$

$$b = -\frac{\tanh^2 \theta_0}{(1 - \tanh^2 \theta_0) (1 + (d - 1) \tanh^2 \theta_0)}. \quad (83)$$

Then, by definition of $\|Q_{S^c S}^* (Q_{SS}^*)^{-1}\|_{\infty}$, according to Lemma 8, it is achieved for $r \in S^c$ where r belongs to the nearest neighbors of the nodes in S . Specifically, in that case, the elements in the row in $Q_{S^c S}^*$ associated with node $r \in S^c$ can only take two different values: one element is $\tanh \theta_0$ and the other $(d - 1)$ elements are $\tanh^3 \theta_0$. Then, from (81), after some algebra, it can be calculated that

$$\|Q_{S^c S}^* (Q_{SS}^*)^{-1}\|_{\infty} = \tanh \theta_0 := 1 - \alpha, \quad (84)$$

where we obtain an analytical result $\alpha := 1 - \tanh \theta_0 \in (0, 1]$, which completes the proof.

References

- Alia Abbara, Yoshiyuki Kabashima, Tomoyuki Obuchi, and Yingying Xu. Learning performance in inverse ising problems with sparse teacher couplings. *Journal of Statistical Mechanics: Theory and Experiment*, 2020(7):073402, 2020.
- Julian Besag. Statistical analysis of non-lattice data. *Journal of the Royal Statistical Society: Series D (The Statistician)*, 24(3):179–195, 1975.
- Aurélien Decelle and Federico Ricci-Tersenghi. Pseudolikelihood decimation algorithm improving the inference of the interaction network in a general class of ising models. *Physical review letters*, 112(7):070603, 2014.
- Arkopal Dutt, Andrey Y Lokhov, Marc Vuffray, and Sidhant Misra. Exponential reduction in sample complexity with learning of ising model dynamics. *arXiv preprint arXiv:2104.00995*, 2021.
- Holger Höfling and Robert Tibshirani. Estimation of sparse binary pairwise markov networks using pseudo-likelihoods. *Journal of Machine Learning Research*, 10(4), 2009.
- Ernst Ising. Beitrag zur theorie des ferromagnetismus. *Zeitschrift für Physik*, 31(1):253–258, 1925.
- Hilbert J. Kappen and Francisco de Borja Rodríguez. Efficient learning in boltzmann machines using linear response theory. *Neural Computation*, 10(5):1137–1156, 1998.
- Daphne Koller and Nir Friedman. *Probabilistic graphical models: principles and techniques*. MIT press, 2009.
- Jeyashree Krishnan, Reza Torabi, Andreas Schuppert, and Edoardo Di Napoli. A modified ising model of barabási–albert network with gene-type spins. *Journal of mathematical biology*, 81(3):769–798, 2020.
- Korbinian Liebl and Martin Zacharias. Accurate modeling of dna conformational flexibility by a multivariate ising model. *Proceedings of the National Academy of Sciences*, 118(15), 2021.
- Andrey Y Lokhov, Marc Vuffray, Sidhant Misra, and Michael Chertkov. Optimal structure and parameter learning of ising models. *Science advances*, 4(3):e1700791, 2018.
- Daniel Marbach, James C Costello, Robert Küffner, Nicole M Vega, Robert J Prill, Diogo M Camacho, Kyle R Allison, Manolis Kellis, James J Collins, and Gustavo Stolovitzky.

- Wisdom of crowds for robust gene network inference. *Nature methods*, 9(8):796–804, 2012.
- Julian J McAuley and Jure Leskovec. Learning to discover social circles in ego networks. volume 2012, pages 548–56. Citeseer, 2012.
- Nicolai Meinshausen, Peter Bühlmann, et al. High-dimensional graphs and variable selection with the lasso. *The annals of statistics*, 34(3):1436–1462, 2006.
- Xiangming Meng, Tomoyuki Obuchi, and Yoshiyuki Kabashima. Structure learning in inverse ising problems using ℓ_2 -regularized linear estimator. *arXiv preprint arXiv:2008.08342*, 2020.
- Xiangming Meng, Tomoyuki Obuchi, and Yoshiyuki Kabashima. Ising model selection using ℓ_1 -regularized linear regression. *arXiv preprint arXiv:2102.03988*, 2021.
- Marc Mezard and Andrea Montanari. *Information, physics, and computation*. Oxford University Press, 2009.
- Marc Mézard, Giorgio Parisi, and Miguel Angel Virasoro. *Spin glass theory and beyond: An Introduction to the Replica Method and Its Applications*, volume 9. World Scientific Publishing Company, 1987.
- Faruck Morcos, Andrea Pagnani, Bryan Lunt, Arianna Bertolino, Debora S Marks, Chris Sander, Riccardo Zecchina, José N Onuchic, Terence Hwa, and Martin Weigt. Direct-coupling analysis of residue coevolution captures native contacts across many protein families. *Proceedings of the National Academy of Sciences*, 108(49):E1293–E1301, 2011.
- Sahand N Negahban, Pradeep Ravikumar, Martin J Wainwright, Bin Yu, et al. A unified framework for high-dimensional analysis of m -estimators with decomposable regularizers. *Statistical science*, 27(4):538–557, 2012.
- H Chau Nguyen and Johannes Berg. Bethe–peierls approximation and the inverse ising problem. *Journal of Statistical Mechanics: Theory and Experiment*, 2012(03):P03004, 2012.
- Hidetoshi Nishimori. *Statistical physics of spin glasses and information processing: an introduction*. Number 111. Clarendon Press, 2001.
- Manfred Opper and David Saad. *Advanced mean field methods: Theory and practice*. MIT press, 2001.
- Matjaž Perc, Jillian J Jordan, David G Rand, Zhen Wang, Stefano Boccaletti, and Attila Szolnoki. Statistical physics of human cooperation. *Physics Reports*, 687:1–51, 2017.

- Pradeep Ravikumar, Martin J Wainwright, John D Lafferty, et al. High-dimensional ising model selection using ℓ_1 -regularized logistic regression. *The Annals of Statistics*, 38(3): 1287–1319, 2010.
- Federico Ricci-Tersenghi. The bethe approximation for solving the inverse ising problem: a comparison with other inference methods. *Journal of Statistical Mechanics: Theory and Experiment*, 2012(08):P08015, 2012.
- R Tyrrell Rockafellar. *Convex analysis*, volume 36. Princeton university press, 1970.
- Stefan Roth and Michael J Black. Fields of experts: A framework for learning image priors. In *2005 IEEE Computer Society Conference on Computer Vision and Pattern Recognition (CVPR'05)*, volume 2, pages 860–867. IEEE, 2005.
- Adam J Rothman, Peter J Bickel, Elizaveta Levina, Ji Zhu, et al. Sparse permutation invariant covariance estimation. *Electronic Journal of Statistics*, 2:494–515, 2008.
- Narayana P Santhanam and Martin J Wainwright. Information-theoretic limits of selecting binary graphical models in high dimensions. *IEEE Transactions on Information Theory*, 58(7):4117–4134, 2012.
- Toshiyuki Tanaka. Mean-field theory of boltzmann machine learning. *Physical Review E*, 58(2):2302, 1998.
- Robert Tibshirani. Regression shrinkage and selection via the lasso. *Journal of the Royal Statistical Society: Series B (Methodological)*, 58(1):267–288, 1996.
- Roman Vershynin. *High-dimensional probability: An introduction with applications in data science*, volume 47. Cambridge university press, 2018.
- Marc Vuffray, Sidhant Misra, Andrey Lokhov, and Michael Chertkov. Interaction screening: Efficient and sample-optimal learning of ising models. In *Advances in Neural Information Processing Systems*, pages 2595–2603, 2016.
- Martin J Wainwright and Michael Irwin Jordan. *Graphical models, exponential families, and variational inference*. Now Publishers Inc, 2008.
- Martin J Wainwright, John D Lafferty, and Pradeep K Ravikumar. High-dimensional graphical model selection using ℓ_1 -regularized logistic regression. In *Advances in neural information processing systems*, pages 1465–1472, 2007.
- Peng Zhao and Bin Yu. On model selection consistency of lasso. *The Journal of Machine Learning Research*, 7:2541–2563, 2006.